Photoelectric Atomic Absorption Cross Sections for Elements Z=6 to 54 in the Medium Energy X-ray Range 5 to 25 keV
Part II

A Comparison with other Theoretical and Experimental Data

J. D. Stephenson

Fritz-Haber-Institut der Max-Planck-Gesellschaft, Berlin-Dahlem, Germany

(Z. Naturforsch. **30 a**, 1133–1142 [1975]; received June 27, 1975)

A comparison is made between recent computations of X-ray photoeffect absorption cross sections, using screened hydrogen-like eigenfunctions, given in Part I[1], and those of an alternate more rigorous theory together with those estimable from experimental X-ray absorption coefficients. Some inherent limitations, which restrict the present results, are discussed. Photoeffect mass absorption coefficients for a limited number of elements between $Z = 10$ and 39 are determined from the hydrogen-like theory, using five characteristic X-ray energies from NiLα 1 (0.852 keV) to TiLα 1 (4.511 keV).

1. Introduction

The aim of this paper is to show that the recent theoretical numerical computation of X-ray photoeffect absorption cross sections[1], calculated by means of hydrogen-like eigenfunctions, is in close agreement with the results of more rigorous theory and those estimable from X-ray linear absorption coefficients. The agreement is particularly good for incident radiation energies in the medium X-ray range 5 to 25 keV, where photoelectric absorption is chiefly confined to the inner K and L atomic subshells. The prior interest in this theory, as discussed in Part I, concerned the determination of (minimum) absorption coefficients[2], related to the anomalous transmission of X-rays through thick perfect crystals (Borrmann effect). For such calculations an accurate knowledge of the atomic dipole and quadrupole components of the total photoelectric absorption cross section is required.

The tables given in[1] are extended in this paper to the 0.8 to 5 and 25 to 30 keV regions to determine acceptable limits for their application. The following sections compare these hydrogen-like results with those of more rigorous theory and experiment.

2. Comparison with Alternate Theory

A major inconsistency in the hydrogen-like theory concerns the disparity which exists between experimental and theoretical absorption edge energies; these were obtained experimentally from the sub-shell energy levels $E(\mathrm{K})$, $E(\mathrm{L})$ ... etc. of Bearden and Burr[3] and theoretically from screened hydrogenlike eigenvalues $E(\mathrm{n,l})$ *. Such differences are best illustrated in Fig. 1, which also shows that a linear relationship exists between the logarithms of the sub-shell absorption edge energies $E(\mathrm{n,l})$, $E(\mathrm{K})$ ... etc. and the logarithm of the element atomic number Z. The differences, separating corresponding theoretical and experimental absorption edges, may be of the order of several hundred eV; they increase with increasing Z.

In order that cross sections between the theoretical $E(n,\mathrm{l})$ and experimental $E(\mathrm{K})$ ... etc. absorption edges of each element may be included, a non rigorous extension to the theory, similar to that used by Hönl[4], has been introduced into our calculations. This form of extension has already shown satisfactory agreement with the experimental results of Persson and Efimov[5] close to the K-absorption edge of germanium and has been described in[2].

2.1. Elements Z = 6, 10, 13, 18, 20, 26, 29, 36, 42, 47 and 50

Table 1 gives hydrogen-like photoeffect cross sections for the elements $Z = 6$, 10, 13, 18, 20, 26, 29, 36, 42, 47 and 50 in comparison with the photo-

* Theoretical hydrogen-like eigenvalues $E(\mathrm{n,l})$, in keV, are determined from $E(\mathrm{n,l}) = 12.3981/\lambda_{\mathrm{nl}}$ where $\lambda_{\mathrm{nl}} = n^2/(Z-s_{\mathrm{nl}})^2$. s_{nl} being the inner screening constant for an electron in an atomic subshell of quantum numbers n and l and λ_{nl}, the wavelength corresponding to the hydrogen-like eigenvalue of this state.

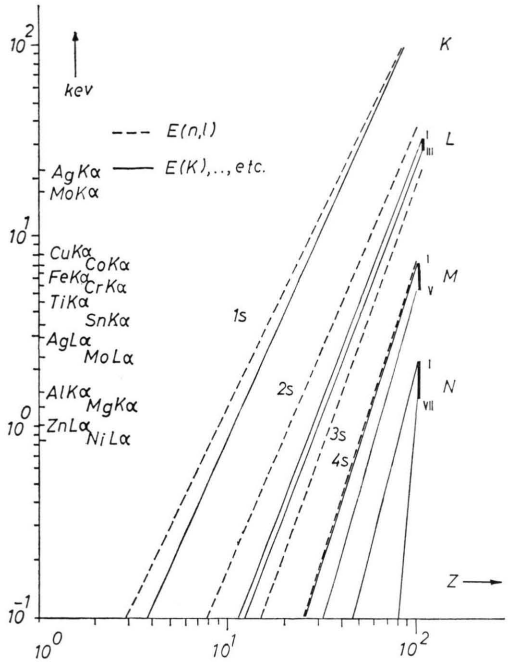

Fig. 1. Hydrogen-like eigenvalues $E(n,l)$, dashed lines, and experimental absorption edge energies, solid lines, given in keV and plotted as a function of atomic number Z. Several characteristic X-ray energies are listed, from which horizontal traces, almost as far as the E(2s) eigenvalue edge, indicate the highest Z elements, for which the hydrogen-like calculations are still found to be useful, e. g. for CrKα the useful range is given by $6 \lesssim Z \lesssim 43$.

ionization cross sections, computed by Scofield[6], using Hartree-Fock-Slater potentials. The incident photon energies considered are 1, 5, 10 and 20 keV. For these cases Scofield's results are treated as a useful standard, since they compare well with those of other alternate theories and with experiment. Their subdivision into the K, L, M and N-shell contributions is convenient for a direct comparison with those, obtained from the screened hydrogen-like theory. Additional comparisons are given in Table 1 for aluminium ($Z = 13$), using the sub-shell cross sections of Brysk and Zerby[7], which are based on Dirac-Slater wavefunctions. Those for elements Fe ($Z = 26$) and Sn ($Z = 50$) by Rakavy and Ron[8], employing a modified Fermi potential method, and the results of Storm and Israel[9], founded on the computer program of Brysk and Zerby, are also included. Additional data, not found in the published articles[7, 8], but given in the comparison of Storm and Israel, are enclosed in brackets together with the notation (SI) behind the author(s) initials. Further absorption cross sections, computed by Schmickley and Pratt[10], using modified Coulomb potentials, are not listed here; they are similar to those of the more rigorous theories. Table 1 shows, that a satisfactory agreement exists between many cross sections in the medium X-ray range, particularly for elements $Z = 10$ to 54. In such regions the close match of the hydrogen-like results is due to their remarkably accurate cross sections in the energy regions, where K- and L-shell absorption predominates. Such inner shell cross sections tend to mask deficiencies in their remaining outer shells; these differences are clearly distinguishable in Figs. 2, where hydrogen-like cross sections (solid lines) are compared with the more rigorous theoretical results of Scofield (dashed lines).

For energies below the medium X-ray energy range Fig. 2 a shows, for 1 keV, that relatively large differences ($\sim 30\%$) exist in regions, extending from the L and M absorption edges; these differences become progressively smaller and less extensive with increased X-ray energies. Comparisons close to such absorption edges must however be considered as tentative, due to Kossel and Kronig-Kramer fine structure. For example the fine structure of metallic copper ($Z = 29$) extends 300 eV from the high energy side of the K-absorption edge and varies the linear absorption coefficient in this region by as much as $\pm 5\%$. Such effects are not accounted for in the above theoretical works.

It is observed from Figs. 2, that an overall satisfactory agreement exists between the hydrogen-like cross sections and those of Scofield, providing one restricts the hydrogen-like calculations to elements, whose Z values lie beneath the dominant parts of the K- and L-shell envelopes. Generally, the useful range of elements, to which the hydrogen-like calculations can be applied successfully in this X-ray energy range, is given by

$$6 \lesssim Z \lesssim Z_{E(2s)},$$

where $Z_{E(2s)}$ is the atomic number of an element, whose 2s electron has a hydrogen-like eigenvalue, closest to the incident X-ray energy. Approximate values for $Z_{E(2s)}$, for a given- X-ray energy, can be obtained directly from Figure 1. The upper Z value in this range is less than $Z_{E(2s)}$ for X-ray energies below 10 keV and almost equal to $Z_{E(2s)}$ for higher energies. A further observation shows, that the theoretical extension, mentioned earlier in Sect. 2,

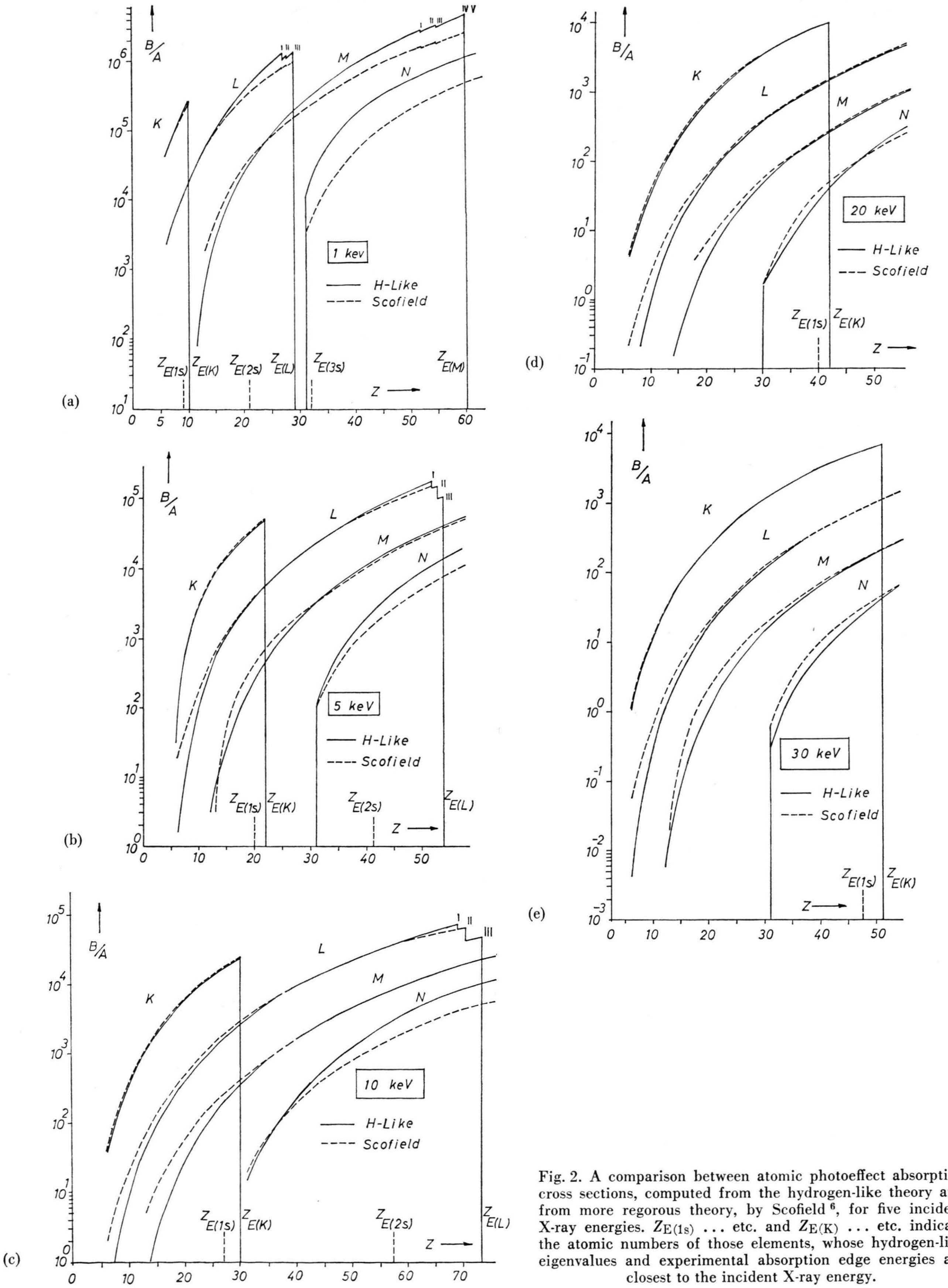

Fig. 2. A comparison between atomic photoeffect absorption cross sections, computed from the hydrogen-like theory and from more regorous theory, by Scofield [6], for five incident X-ray energies. $Z_{E(1s)}$ ... etc. and $Z_{E(K)}$ ... etc. indicate the atomic numbers of those elements, whose hydrogen-like eigenvalues and experimental absorption edge energies are closest to the incident X-ray energy.

Table 1. Photoelectric hydrogen-like and alternative theoretical atomic absorption cross sections in barn/atom (S – Scofield [6], BZ – Brysk and Zerby [7], SI – Storm and Israel [9], RR – Rakavy and Ron [9]). Bracketed H-like values are doubtful; bracketed alternate theory values are taken from Storm and Israel [9].

	keV		1.0					5.0		
	Z	K	L	M	τ	K	L	M	N	τ
C	6	40390	(277)	—	40667	315.8	(1.59)	—	—	317.4
		42045	2028	—	44073	353.9	18.2	—	—	372.1
					43500					371.0
Ne	10	256500	11195	—	267695	2849	84.4	—	—	2933
		232060	16051	—	248111	2924	171.0	—	—	3095
					252000					3100
Al	13	—	47620	(689)	48309	8040	399.5	(5.4)	—	8445
		—	51060	1941	53001	7996	581	33.9	—	8611
					(52500)					(8460)
			43972		(44000)	7862	513			(8380)
Ar	18	—	210430	13450	223880	26280	1956	117	—	28353
		—	193830	17171	211001	25224	2425	251	—	27900
					205000					28100
Ca	20	>10% difference				37520	3350	247	—	41117
						35560	3782	466	—	39808
										40000
Fe	26					—	11515	1244	—	12759
						—	11177	1507	—	12684
						—	10452	1181	—	11633
										12500
Cu	29					—	17215	1871	—	19088
						—	17349	2354	—	19703
										19500
Kr	36					—	41060	6577	869	48510
							40261	6359	577	47197
										47000
Mo	42					—	77300	13800	2937	94037
						—	71603	12823	1736	86162
										86000
Ag	47					—	118090	22400	6204	146694
						—	107060	20999	3310	131369
										132000
Sn	50					—	148490	29490	8982	186962
						—	132820	27374	4896	165090
						—	131650	26203	3147	161000
										165000

is found to be suitable only for the $E(\mathrm{K})$ absorption edge region and not for the subsequent $E(2\mathrm{s})$ to $E(\mathrm{L})$ and $E(3\mathrm{s})$ to $E(\mathrm{M})$ regions, where hydrogen-like cross sections are generally 10% or more greater than those of experiment and alternate theory.

In Fig. 2 relatively large differences are observed between the initial (low Z) L, M, and N absorption cross sections, obtained from the two theoretical approaches; they chiefly concern elements, which have an incompletely filled outer sub-shell. Such differences may be due to an approximation made in the hydrogen-like calculations of Part I, in which screening constants for incomplete sub-shells were taken from averages of their calculable full shell values. An approximation of this kind was required due to a lack of experimental term differences, necessary for their evaluation by the usual Sommerfeld method; this method has been described in Part I. In such cases the approximation tends to slightly overestimate the value of the screening constants of these shells, resulting in smaller absorption cross sections than are possible, using more precise screening constants. Fortunately, for medium Z elements alternate theory indicates, that such incomplete shells contribute less than 1% to the total cross section. It is however more serious for low atomic number elements, such as carbon ($Z=6$), whose L-shell contribution is of the order of 5%. The cross sections of incomplete shells, given in Table 1, are therefore doubtful and are enclosed in brackets. Alternative screening constants for low atomic num-

Tabelle 1, Fortsetzung.

		10.0						20.0		
K	L	M	N	τ	K	L	M	N	τ	Ref.
35.2	(0.16)	—	—	35.36	3.79	(0.01)	—	—	3.8	H-like
39.3	2.0	—	—	41.3	4.1	0.2	—	—	4.3	S
				39.3					4.14	SI
352	9.6	—	—	361.6	41.3	1.0	—	—	42.3	H-like
362	21.	—	—	383	41.6	2.4	—	—	44	S
				386					42.9	SI
1063	(47.9)	—	—	1111	131.6	5.5	(0.06)	—	137.2	H-like
1064	75.1	—	—	1139	129.3	9.0	0.61	—	138.9	S
1066	75.3	—	—	1141					(137)	BZ (SI)
1036	66.8	—	—	1103					(129)	RR (SI)
3848	248	14	—	4110	516	31	1.9	—	548.9	H-like
3769	329	35	—	4133	498	42	4.6	—	544.6	S
				4100					537	SI
5707	431	31	—	6169	789	54	3.7	—	846.7	H-like
5558	520	66	—	6144	758	67	8.7	—	833.7	S
				6100					824	SI
14390	1534	163	—	16087	2167	200.5	28.4	—	2396	H-like
13847	1586	219	—	15652	2078	213	30.2	—	2321	S
13940	1481	176	—	15597					(2340)	RR (SI)
				15700					2310	SI
20610	2319	301	—	23230	3230	307	40	—	3577	H-like
19765	2493	348	—	22606	3103	339	48	—	3490	S
				22600					3480	SI
—	5693	908	96	6697	6813	772	122	10	7717	H-like
—	5992	955	97	7044	6582	839	135	15	7571	S
				6820					7570	SI
—	11012	1944	347	13303	11140	1524	266	37.8	12968	H-like
—	11042	1954	293	13289	10590	1584	281	44.7	12500	S
				13100					1910	SI
—	17204	3182	784	21170		2418	440	89	2947	H-like
—	17096	3247	550	20893		2505	473	64	3042	S
				20600					3020	SI
—	21946	4206	1182	27334		3112	584	137	3833	H-like
—	21647	4270	817	26734		3216	628	127	3971	S
	21319	4092	189	25600					(3730)	RR (SI)
				26400					3910	SI

ber elements $Z = 3$ to 10 have been given by Duncanson and Coulson [11]. Substitution of these values into our calculations gives improvements in L-shell cross sections, relative to Scofield, at the expense of lower K-shell values. The net effect gives total cross sections, which are not substantially different from the hydrogen-like results, given in [1], and have therefore not been found useful for this energy range.

3. Comparisons with Experiment

3.1. Linear Absorption

In this section comparisons are made between the *photoeffect* mass absorption coefficients (τ/ϱ), calculated from the hydrogen-like theory, and *experimental* mass absorption coefficients (μ/ϱ). Theoretical estimates of the coherent and incoherent scattering, inherent in the experimental coefficients, are given tentatively in brackets near each hydrogen-like value and marked with a triangle ▲; these values are estimated from tables, given by Storm and Israel [9], and should be added to the hydrogen-like coefficients for comparison purposes.

3.1.1. Elements Ne, Ar, Kr and Xe

Table 2 gives hydrogen-like photoeffect mass absorption coefficients for the rare earth gases Ne(10), Ar (18), Kr (36) and Xe (54) in comparison with those measured experimentally by Wuilleumier [12], Bearden [13], and Chipman and Jennings [14]. A limited number of compiled theoretical/experimental coefficients from the revised edition of the International Tables (Vol. IV) is also included. Of these results

Table 2. Hydrogen-like photoeffect mass absorption coefficents (τ/ϱ), compared with the experimental mass absorption coefficients (μ/ϱ), given by Wuilleumier [12]. Experimental coefficients, measured by B – Bearden [13] and C & J – Chipman and Jennings [14], are also included together with the compiled theoretical/experimental coefficients, recently listed in the International Tables [15] (Vol. IV). The additional scattering, due to Compton and thermal diffuse scattering etc., estimated from Storm and Israel [9], is marked with a triangle – ▲. Bearden's cross sections, in barn/atom, have been reconverted to cm^2/g, using the conversion factors 0.029840 (cm^2/g)/(barn/atom) for Ne and 0.015080 (cm^2/g)/(barn/atom) for Ar.

Line	keV	Ne (10) Expt.	Ne (10) H-like	Ne ▲	Ne I.T.	Ar (18) Expt.	Ar (18) H-like	Ar ▲	Ar I.T.
AgKα1	22.163	— +)	0.917	(0.3)	1.163	—	6.10		6.28
MoKα1	17.479	2.0 ± 0.4 (CJ)	1.92	(0.4)	2.209	12.2 ± 0.3 (CJ)	12.29		12.62
	8.249	—	19.43			—	107.0		
CuKα1	8.048	22.0 ± 0.2 (B)	20.94	(0.6)	22.13	118.1 ± 1 (B)	114.7	(1.0)	119.5
	7.982	—	21.47			—	117.4		
	7.733	—	23.64			—	128.3		
CoKα1	6.930	—	32.93		32.69	—	174.4		180.9
FeKα1	6.404	44.7 ± 0.4 (B)	41.78		44.0	214.4 ± 3 (B)	217.1		225.1
	6.186	45.5 ± 1	46.35			248 ± 12	238.8	(1.3)	
CrKα1	5.415	76.1 ± 0.7 (B)	69.05		72.71	422 ± 4 (B)	344.3		355.5
	5.265	81.1 ± 2	75.06			374 ± 19	371.6		
	5.050	91.5 ± 5	84.96	(1.0)		—	416.1	(1.5)	
	4.759	108 ± 3	101.3			545 ± 33	488.7		
	4.669	114 ± 5	107.2			114 ± 5	107.2		
TiKα1	4.511	130 ± 1 (B)	118.7		124.8	665 ± 7	564.4		576.9
	4.266	152 ± 5	139.9			152 ± 5	139.9	…………	E (1s)
	3.991	186 ± 7	170.1	(1.2)		186 ± 7	170.1	(1.7)	
	3.639	236 ± 7	222.9			236 ± 7	222.9		
	3.535	250 ± 10	242.5			1119 ± 45	1097		
SnLα1	3.444	282 ± 5 (B)	261.6			1468 ± 29 (B)	1156		
	3.299	300 ± 12	296.3			300 ± 12	296.3	———	K
AgLα1	2.984	420 ± 8 (B)	395.9	(1.5)		203 ± 4	143.1	(2.1)	
	2.981	401 ± 16	396.9			179 ± 9	143.5		
	2.605	583 ± 18	584.1			247 ± 7	213.0		
	2.313	808 ± 32	818.4			316 ± 16	301.5		
MoLα1	2.293	770 ± 15 (B)	838.2	(1.7)		307 ± 6 (B)	309.1		
	2.000	—	1229			—	460.1	(2.6)	
	1.996	1235 ± 74	1237			504 ± 30	463.0		
	1.900	1392 ± 56	1418			—	533.9		
	1.800	1617 ± 49	1647			670 ± 33	624.6		
	1.700	1872 ± 56	1927			795 ± 40	736.9		
	1.672	1965 ± 98	2018			840 ± 50	773.2		
	1.600	2253 ± 112	2276			961 ± 58	878.1		
AlKβ	1.557	2417 ± 72 (B)	2451			1040 ± 31 (B)	949.9	(2.8)	
	1.556	—	2456	(1.8)		—	951.6		
AlKα1	1.487	2754 ± 82 (B)	2778			1149 ± 34 (B)	1084		
MgKα1	1.254	4327 ± 130 (B)	4394	…………	E (1s)	1764 ± 53 (B)	1770		
ZnLα1	1.012	7698 ± 230 (B)	7744			3197 ± 96 (B)	3263		
CuLα1	0.930	9817 ± 290 (B)	9652	———	K	4041 ± 120 (B)	4147		
NiLα1	0.852	746 ± 22 (B)	537.0	(1.9)		4599 ± 140 (B)	5311	(3.0)	

+ Misprinted as 20 ± 0.4 in original article [14] (L. D. Jennings, private communication).

those of Wuilleumier, using the continuous Bremsstrahlung radiation from the tungsten target of an X-ray tube, are particularly useful for comparisons in the low X-ray energy range 0.8 to 8 keV. Such measurements are almost continuous and transgress one or more experimental absorption edges with decreasing X-ray energy; these edges are readily obtained from Fig. 1, by constructing vertical traces from the Z values. As each K, L, M, and N absorption edge is passed, the cross sections of the remanent (L + M . . .), (M + N . . .) etc. shell contributions are revealed; these values are useful in assessing the nonhydrogenic behaviour of the outer shell cross sections, given in [1]. For example, comparisons below the L_{III} edges of Kr and Xe show, that the hydrogen-like (M + N . . .) contributions are 20% higher than those of experiment. Such large differences may be due almost entirely to the non hydrogenic character of the outer M and N-shells, although to some extent such differences may be

Tabelle 2, Fortsetzung.

Kr (36) Expt.	Kr (36) H-like	▲	Kr (36) I.T.	Xe (54) Expt.	Xe (54) H-like	▲	Xe (54) I.T.
	42.17	(0.7)	42.53		18.25	(1.4)	20.01
79.9 ± 0.2 (CJ)	79.23	K	79.10	38.39 ± 0.13 (CJ)	35.74	(1.9)	38.31
97 ± 4	83.68	(2.4)	97.02	275 ± 12	293.8	(3.9)	E (2s)
—	89.81			—	314.6		309.8
102 ± 5	91.94			300 ± 13	321.7		
110 ± 5	100.7			327 ± 10	351.2		
—	137.8		145.7	—	474.9		459.0
—	172.6		180.7	—	589.8	(4.4)	564.0
202 ± 11	190.5	(3.4)		592 ± 28	648.2		L_I
—	278.1		284.6				
316 ± 16	301.1						
354 ± 15	338.9	(4.0)					
411 ± 17	400.9						
435 ± 22	423.0						
—	466.1		464.3				
—	—						
548 ± 23	545.3						
653 ± 21	657.6	(4.0)					
809 ± 25	851.6		E (2s)				
870 ± 36	923.4						
—	993.0						
1040 ± 50	1478	(4.5)					
—	—						
1360 ± 60	1482						
1970 ± 90	2149						
2680 ± 30	2974						
—	3044						
—	4409						
3840 ± 120	4436		L_I				

exaggerated by using inaccurate (low) screening constants.

Agreement between the hydrogen-like and experimental coefficients, in many cases within 5%, is however possible, so long as the hydrogen-like calculations are again restricted to X-ray energies above the theoretical $E(2s)$ eigenvalue of the element concerned. As an example in using energies lower than this value, the coefficients for Kr and Xe, given in Table 2, are extended to the lower L_I absorption edges; these extensions show, that one can expect differences between theory and experiment of the order of 10% and greater in these regions.

3.1.2. Al and the Transition Metals

For aluminium and the transition metals Ti, V, Cr, Mn, Ni, Fe, Cu, and Zn comparisons in the medium energy X-ray range are made with the experimental mass absorption coefficients of Heinrich[16], Bearden[17], Middleton and Gazzara[18], Cooper[19], Hughes, Woodhouse and Bucklow[20] and Andrews[21] together with some of the recent low energy results by Singman[22] in the range 1.4 to

Table 3. Hydrogen-like photoeffect mass absorption coefficients (τ/ϱ) in cm²/g compared with experimental linear mass absorption coefficients (μ/ϱ). Theor.: H-like (Hildebrandt, Stephenson, Wagenfeld)[1]; Exper.: A (Andrews)[21]; B (Bearden)[13]; HWB (Hughes, Woodhouse and Bucklow)[20]; H (Heinrich)[16]; MG (Middleton & Gazzara)[18]; Sn (Singman)[22]; Theor./Exper.: I. T. (International Tables; Vol. IV5[15]; Theor.: ▲ (other Scattering)[9]. Bracketed values are to be considered as tentative.

	keV	AlKα1 1.487		AgLα1 2.984			CrKα1 5.415		FeKα1 6.404	
	Z	H-like	Expt.	H-like	Expt.	Ref.	H-like	Expt.	H-like	Expt.
Al	13	337	396±16	804	793±32	Sn	149.9	156.0±3.7	92.23	96.8±1.2
			415		804			149.5±0.9		92.1±0.6
								149		92.4
		▲ (2.0)		▲ (1.5)	822	A	▲ (1.2)	158	▲ (1.0)	97.54
Ti	22	2454	2246±90	336	342±14	Sn	(582.5)	—	373.3	—
					345			593		377
										—
		▲ (3.4)		▲ (2.6)			▲ (1.9)	571.4	▲ (1.6)	370.1
V	23			394			70.03	82.7 ±2.8	(409.9)	387.7±7.0
				(2.7)			▲ (2.0)	75.06	▲ (1.7)	411.4
Cr	24			468			83.65	(88.7)	(464.1)	—
				▲ (3.0)			▲ (2.2)	85.71	▲ (1.9)	462.2
Mn	25			528			94.99	(99.1)	58.30	(61.1)
				▲ (3.1)			▲ (2.2)	96.08	▲ (1.9)	59.93
Fe	26			606	582±23	Sn	105.5	112.2±1.8	67.25	69.7±1.1
									▲ (2.1)	70.40
				▲ (3.4)			▲ (2.5)	113.1	73.72	78.0±0.6
Co	27			660			120.0	(126.0)	▲ (2.2)	78.29
				▲ (3.6)			▲ (2.6)	124.6		91.5±1.5
Na	28			759	745±30	Sn	138.5	146.5±2.3	85.18	92.0
					738			145.7	▲ (2.5)	91.76
				▲ (3.9)			▲ (2.9)	145.7		96.0±1.5
Cu	29			804	806±32	Sn	147.7	154.5±2.5	90.89	—
					778					
					773	A		155		96.7
				▲ (3.9)			▲ (3.0)	155.2	▲ (2.6)	97.36

3 keV. Table 3 compares these experimental coefficients with the *photoelectric* coefficients of the hydrogen-like theory; additional compiled coefficients from the revised edition of the International Tables[15] (Vol. IV) are also given. Theoretical estimates of the coherent and incoherent scattering[9], to be added to the hydrogen-like values for comparison purposes, are included in brackets and marked with a triangle ▲. The agreement with experiment for these medium Z elements in the medium X-ray energy range is shown to be particularly good. Alternate theoretical photoeffect coefficients for these elements, using several medium X-ray energies, have also been computed relativistically by Cromer and Liberman[23]; they are generally within 3% of our hydrogen-like results.

3.1.3. Soft X-ray Mass Absorption Coefficients for Elements $Z=10$ to 39

Since measurements of mass absorption coefficients in the soft X-ray energy region are relatively few, several hydrogen-like photoeffect mass absorption coefficients are given in Table 4 for five characteristic X-ray energies between TiLα1 (4.511 keV) and NiLα1 (0.852 keV). Such values are restricted to elements $Z=10$ to 39 and curtailed at X-ray energies a little higher than the theoretical $E(2s)$ eigenvalues. The additional contributions of coherent and incoherent scattering, estimated from [9], are quite small and generally less than 1%.

3.2. Anomalous Absorption

The anomalous transmission of X-rays, diffracted through thick perfect crystals (Borrmann effect), has been shown by Wagenfeld[24] to have a small angular dependence on the quadrupole component of the total photoelectric absorption (at room temperature, however, this dependence is secondary to the influence of the Debye-Waller factor). Such quadrupole contributions are directly proportional to the values of "Q", given in the tables of Part I.

To some extent the experimental results of [2] have confirmed the existence of the quadrupole contribution to the anomalous absorption of X-rays in ger-

Tabelle 3, Fortsetzung.

H-like	CoKα1 6.931 Expt.	H-like	CuKα1 8.048 Exp.	H-like	MoKα1 17.479 Exp.	H-like	AgKα1 22.163 Expt.	Ref.
92.23	76.19 ± 0.85	47.23	50.40 ± 0.57	4.62	5.10 ± 0.02	2.24	2.65 ± 0.01	C
			49.1 ± 1.0					H
			51.6					B
▲ (0.8)	77.54	▲ (0.8)	50.23	▲ (0.4)	5.043	▲ (0.34)	2.54	I.T.
302.1	—	201.7	(187.5)	23.06	(22.23)	11.66	(11.53)	C
			206		—		—	HBW
			—		—		11.78 ± 0.05	MG
▲ (1.5)	300.5	▲ (1.2)	202.4	▲ (0.7)	23.25	▲ (0.53)	11.76	I.T.
(332.2)	315.6 ± 5.7	222.5	213.9 ± 3.8	25.84	25.18 ± 0.14	13.11	13.71 ± 0.08	C
▲ (1.5)	332.7	▲ (1.3)	222.6	▲ (0.7)	25.24	▲ (0.53)	12.78	I.T.
(376.8)	—	253.1	(246.6)	29.84	(28.84)	15.20	15.18 ± 0.15	C
▲ (1.6)	375.0	▲ (1.4)	252.3	▲ (0.8)	29.25	▲ (0.57)	14.88	I.T.
(409.3)		275.7	(274.2)	32.99	(32.14)	16.87	(16.67)	C
▲ (1.8)	405.1	▲ (1.5)					16.74 ± 0.1	MG
			272.5	▲ (0.8)	31.86	▲ (0.60)	16.23	I.T.
53.43	56.45 ± 0.4	(309.4)	314.3 ± 6.9	37.56	37.61 ± 0.33	19.28	19.38 ± 0.1	C
▲ (1.8)							19.29 ± 0.1	MG
	56.25	▲ (1.6)	304.4	▲ (0.9)	37.74	▲ (0.63)	19.31	I.T.
56.60	61.56 ± 0.5	(331.9)	(350.0)	40.88	40.40 ± 0.32	21.07	21.14 ± 0.11	C
▲ (1.8)	62.86	▲ (1.7)	338.6	▲ (0.9)	41.02	▲ (0.65)	20.92	I.T.
67.73	72.8 ± 1.2	43.86	48.96 ± 0.41	46.82	46.41 ± 0.36	24.23	24.45 ± 0.13	C
			—					HBW
▲ (2.1)	73.75	▲ (1.9)	48.83	▲ (1.0)	47.24	▲ (0.71)	24.32	I.T.
72.29	77.2 ± 1.2	46.85	51.84 ± 0.43	49.10	48.88 ± 0.78	25.50	25.64 ± 0.14	C
			52.2				—	HBW
			50.0				—	A
▲ (2.2)	78.11	▲ (1.9)	51.54	▲ (1.0)	**49.34**	▲ (0.71)	**25.52**	I.T.

manium for several low order reflections. Alternative measurements by Ludewig [25] have also verified its existence in the temperature range $5\,\mathrm{K} \leqq T \leqq 300\,\mathrm{K}$. Comments concerning other experimental work and additional second order contributions to the anomalous absorption have been recently published by Hildebrandt, Stephenson and Wagenfeld [26].

4. Conclusion

The accuracy of our total hydrogen-like photoeffect cross sections, given in the tables of Part I, are in many cases shown to be within 5% of those of the alternate theory and experiment.

This agreement is particularly satisfactory for medium Z elements in the usual X-ray energy range 5 to 25 keV, providing energies are used which are slightly higher than the $E(2s)$ eigenvalue of the element concerned.

Preliminary experimental evidence for germanium [2], using several characteristic X-ray wavelengths, indicates that the values of "Q", given in Part I, are of the correct magnitude. At the present time this is unconfirmed in other perfect crystals, due to insufficient experimental determinations of (minimum) anomalous absorption coefficients.

[1] G. Hildebrandt, J. D. Stephenson, and H. Wagenfeld, Z. Naturforsch. **30 a**, 697 [1975].
[2] G. Hildebrandt, J. D. Stephenson, and H. Wagenfeld, Z. Naturforsch. **28 a**, 588 [1973].
[3] J. A. Bearden and A. F. Burr, Rev. Mod. Phys. **39**, 125 [1967].
[4] H. Hönl, Z. Phys. **84**, 14 [1933].
[5] E. Persson and O. E. Efimov, Phys. Stat. Sol. (a) **2**, 757 [1970].
[6] J. H. Scofield, U. of Calif. Radn. Lab. Report N° 51326 [1973], unpublished; partly published by R. H. Pratt, A. Ron, and H. K. Tseng, Rev. Mod. Phys. **45**, 273 [1973].
[7] H. Brysk and C. D. Zerby, Phys. Rev. **171** (2), 292 [1968].
[8] G. Rakavy and A. Ron, Phys. Rev. **159** (1), 50 [1967].
[9] E. Storm and H. J. Israel, Nuclear Data Tables **A 7**, 565 [1970].
[10] R. Schmickley and R. Pratt, Phys. Rev. **164**, 104 [1967].

Table 4. Hydrogen-like (photoeffect) mass absorption coefficients for elements $Z=10$ to 39 in the soft X-ray region 0.8 to 4.5 keV. The contribution due to other scattering is generally less than 1%.

Z	NiLα1 0.852	CuLα1 0.930	ZnLα1 1.012	MgKα1 1.254	AlKα1 1.487	AlKβ 1.557	MoLα1 2.293	AgLα1 2.984	SnLα1 3.444	TiKα1 4.511	keV
10	537	9651	7743	4394	2778	2451	838	396	262	119	cm^2/g
11	808	624	487	5364	3419	3024	1053	504	335	153	
12	1226	950	741	395	4363	3866	1370	663	443	205	
13	1717	1331	1041	557	337	295	1645	804	541	253	
14	2327	1806	1414	758	461	403	2043	1008	682	322	
15	3317	2580	2024	1089	664	581	2364	1176	799	381	
16	3919	3051	2395	1292	789	690	223	1410	962	463	
17	4682	3651	2869	1552	950	831	270	1566	1073	520	
18		4146	3263	1769	1084	950	309	143	1155	564	
19			4331	2358	1448	1269	415	193	127	696	
20				2962	1824	1600	526	245	161	812	
21				3233	1997	1752	578	270	178	852	
22					2454	2155	716	336	222	101	K
23						2509	839	394	260	119	
24							993	468	310	142	
25							1118	528	350	161	
26							1278	606	402	185	
27							1390	660	439	202	
28							1593	759	505	233	
29								804	536	248	
30								896	598	277	
31								976	652	304	
32								1059	709	330	
33									797	373	
34									853	399	
35										442	
36										466	
										524	
										570	
										626	
										E (2s)	

[11] W. E. Duncanson and C. A. Coulson, Proc. Roy. Soc. (Edin.) **62,** 37 [1944].

[12] F. Wuilleumier, Phys. Paris **26,** 776 [1965]; Phys. Rev. **6,** 2067 [1972].

[13] A. J. Bearden, J. Appl. Phys. **4,** 1681 [1966].

[14] D. R. Chipman and L. D. Jennings, Phys. Rev. **132** (2), 728 [1963].

[15] International Tables for X-ray Crystallography, Vol. IV, Birmingham 1974.

[16] K. F. J. Heinrich, The Electron Probe, J. Wiley, New York 1966, p. 296.

[17] A. J. Bearden, Bull. Amer. Phys. Soc. **4,** 66 [1956].

[18] R. M. Middleton and C. P. Gazzara, Acta Cryst. **23,** 712 [1967].

[19] M. J. Cooper, Acta Cryst. **18,** 813 [1965].

[20] G. D. Hughes, J. B. Woodhouse, and I. A. Bucklow, Brit. J. Appl. Phys. **2** (1), 695 [1968].

[21] C. L. Andrews, Phys. Rev. **54,** 994 [1938].

[22] L. Singman, J. Appl. Phys. **45** (4), 1885 [1974].

[23] D. Cromer and D. Liberman, J. Chem. Phys. **53,** 1891 [1970].

[24] H. Wagenfeld, Phys. Rev. **144** (1), 216 [1966].

[25] J. Ludewig, Z. Naturforsch. **28 a,** 1204 [1973].

[26] G. Hildebrandt, J. D. Stephenson, and H. Wagenfeld, Phys. Stat. Sol. (a) **30,** K 49 [1975].